Method evaluation for analysis of microplastic traces in environmental samples using TD-PTR-TOF-MS

Bachelor thesis

Marnick Anten, 5975638

Natuur- en Sterrenkunde

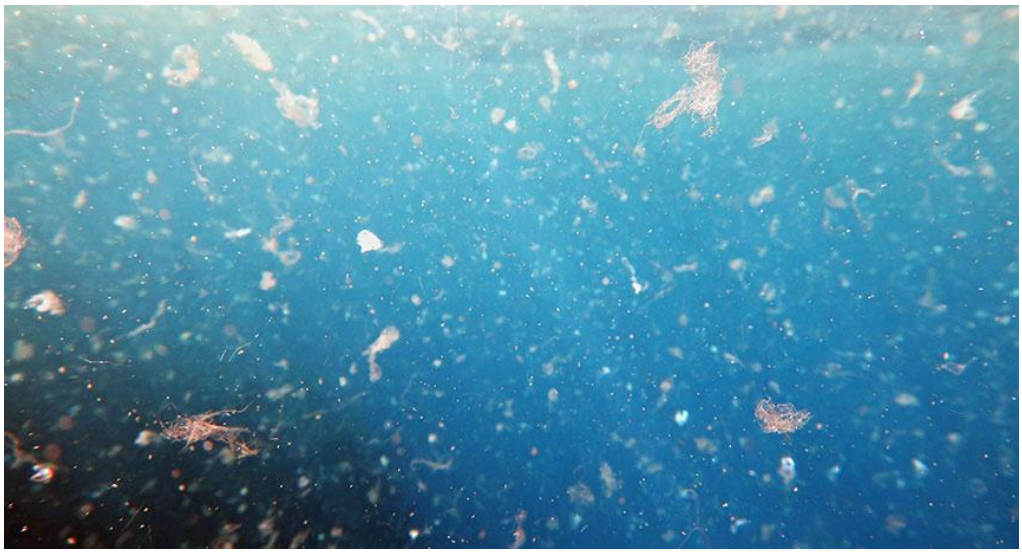

Supervisors:
Dr. D. Materić
Marine and Atmospheric Research Utrecht (IMAU)
Prof. Dr. R. Holzinger
Marine and Atmospheric Research Utrecht (IMAU)
June 12, 2019

Abstract

Plastic that is dumped into the ocean slowly degrades into smaller fragments called microplastics (<5 mm) and nanoplastics (<1 μm). Microplastics as carriers of persistent organic pollutants are a potential risk to humans who ingest up to 52000 microplastic particles annually. Therefore, risk assessment of these small plastic particles is of great importance. The currently available methods have great drawbacks and produce data that is not intercomparable. In this thesis we test a method for analysis of trace components of microplastics in environmental samples using a proton-transfer-reaction time-of-flight mass spectrometer (PTR-TOF-MS). We find that PTR-MS can detect polystyrene at a detection limit of 1 ng. It can detect the ion with m/z=105.069 at concentrations of less than 1 ppb with errors lower than 7%. The PTR-MS can also distinguish between polystyrene (PS), low density polyethylene (LDPE), polyvinyl chloride (PVC) and polyethylene terephthalate (PET).

This means that the PTR-TOR-MS could be used to identify various plastics in environmental samples.

Contents

1.Introduction

Plastic waste is one of this generation's major environmental issues. In the year 2016, 275 million metric tons of plastic waste were produced, of which 4.8 to 12.7 million entered the ocean.[1] Once in the ocean, the plastic starts to degrade into smaller fragments called microplastics (<5 mm) and nanoplastics (<1 µm).[2] [3] These particles end up in not only our oceans, but are also found in human living spaces and even a pristine mountain catchment in the French Pyrenees.[4] [5] This is potentially troublesome because these microplastics can carry high concentrations of persistent organic pollutants.[6] In addition to this, a study has shown a human ingests up to 52000 microplastic particles annually[7]. It is therefore critical for the risk assessment of these microplastics that they can be identified and quantified.

Currently, the main methods for identification of microplastics are Pyrolysis-GC-MS, and FTIR and Raman spectroscopy. However, these methods have their drawbacks. Pyrolysis-GC-MS can only be used to identify the polymer type of the measured plastic, and can only measure one particle at a time.[8] FTIR spectroscopy can only measure particles larger than ~20 µm without significantly underestimating the amount of particles.[9] Raman spectroscopy can measure particles of sizes down to just 1 µm however, measuring a patch of only (1000 x 1000 µm) can take more than a full day.[10]

From these drawbacks, and the problem of intercomparability of data from the current methods, it is clear that a new method for microplastic measurements is needed. [11]

The main goal of this project is to test a method for analysis of microplastic traces in environmental samples by using Proton Transfer Reaction Mass Spectrometry (PTR-MS), and to determine whether microplastics can be found in samples of drinking water and surface snow from the Alps. PTR-MS is a novel method for analysis of microplastic traces in air. It has previously been used to measure aquatic dissolved organic matter, so analysis of microplastic traces is a natural extension of the method.[12]

PTR-MS is chosen because it allows for on-line measuring of a wide range of ions in a sample, with a detection limit in the <1 ppb range. All of this takes as little as fifteen minutes per sample and is independent of particle size as long as the plastic mass is not so high that the sample contaminates the system. The PTR-MS apparatus was able to detect polystyrene (PS) at a detection limit as low as one nanogram. The PTR-MS system was also able to detect and distinguish between PS, PET, LDPE, and PVC by identifying characteristic ions for each plastic, and through principal component analysis.

---

[1] Li, Tse, and Fok, "Plastic Waste in the Marine Environment."
[2] Webb et al., "Plastic Degradation and Its Environmental Implications with Special Reference to Poly(Ethylene Terephthalate)."
[3] Jambeck et al., "Plastic Waste Inputs from Land into the Ocean."
[4] Dris et al., "First Overview of Microplastics in Indoor and Outdoor Air."
[5] Allen et al., "Atmospheric Transport and Deposition of Microplastics in a Remote Mountain Catchment."
[6] Andrady, "Microplastics in the Marine Environment."
[7] Cox et al., "Human Consumption of Microplastics."
[8] Löder and Gerdts, "Methodology Used for the Detection and Identification of Microplastics—A Critical Appraisal."
[9] Käppler et al., "Analysis of Environmental Microplastics by Vibrational Microspectroscopy."
[10] Käppler et al., "Analysis of Environmental Microplastics by Vibrational Microspectroscopy."
[11] Bauerlein et al., "Closing the gap between small and smaller: Towards a framework to analyse nano- and microplastics in aqueous environmental samples."
[12] Peacock et al., "Understanding Dissolved Organic Matter Reactivity and Composition in Lakes and Streams Using Proton-Transfer-Reaction Mass Spectrometry (PTR-MS)."

TD-PTR-TOF-MS

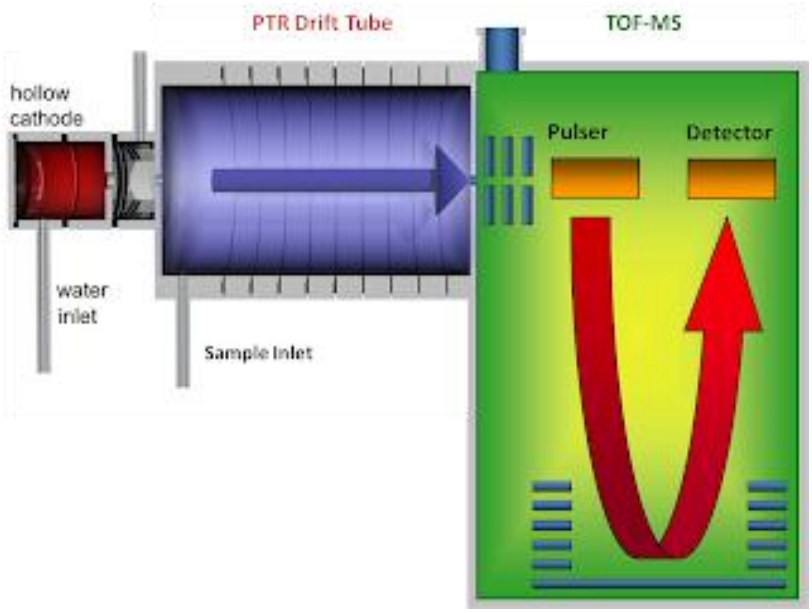

Figure 1: Instrument Schematic of the PTR-TOF-MS

1.1Thermal Desorption

The journey of a sample through the TD-PTR-TOF-MS system starts at the thermal desorption (TD) unit. Here, the sample is gradually heated from 35^{o} C to 350^{o} C. Once the temperature rises above a certain sample-specific temperature, it desorbs from its container into the carrier gas that is being pumped through the said container. For measuring organic compounds the carrier gas has to be nonreactive and devoid of hydrocarbon. In this experiment, the carrier gas was usually zero air, but for one set of measurements, we used nitrogen. Once the sample has desorbed into the carrier gas, it goes into the PTR8000 (Ionicon analitik, Austria) apparatus through the inlet, which is always at a steady 180^{o} C. The inlet is this hot to prevent the sample from sticking to the walls.

1.2 Proton Transfer Reaction

The heated inlet leads the sample to the drift tube, where it is introduced to the hydronium. This hydronium comes from the hollow cathode, where water is turned into plasma. Extremely pure hydronium comes from this plasma into the drift tube, where the following ionization reaction happens between sample and hydronium:

$$H_3O^+ + R \rightarrow H_2O + RH^+ \qquad (1)$$

This reaction is called a proton transfer reaction (PTR). In this reaction an H^+ ion is transferred from the hydronium (H_3O^+) ion onto the sample (R), giving it a charge of +1 and adding one atomic mass unit to its

mass. The benefit of this type of ionization is that it causes much less fragmentation in the sample. This is good because some information is lost when the sample fragments into smaller ions. The proton transfer reaction can happen as long as the sample has a higher affinity for H^+ than both the hydronium and the carrier gas. For most organic compounds this is the case, which allows them to be ionized via this method. Also, hydronium reacts with none of the common constituents of air, which makes air a good carrier gas.[13] A drawback of PTR ionization is that the ions can cluster together. To remedy this, an energizing electric field is applied to the drift tube which gives the ions within it a certain kinetic energy. Particles with high energy are less likely to cluster, but they are also more likely to collide with each other and fragment that way. Balancing the E/N of the particles is therefore crucial for minimizing both the fragmentation and clustering of sample ions. An E/N of about 120 is used throughout this project.[14] Once the sample ions have moved through the drift tube, they get to the time of flight mass spectrometer (TOF-MS). Here a bunch of ions is pulsed into a vacuum at a frequency of about 80 kHz.[15] In this vacuum, an electric and a magnetic field are present, which alter the paths of the ions. Because ions with a higher mass to charge (m/z) ratio are accelerated less by the fields, they take longer to reach the detector. For PTR-MS the charge of the ions is always +1, so we can freely think of this m/z ratio as the actual mass of the ion. Thanks to the fact that ions of different weight take different amounts of time to reach the detector, the ions can be split by mass based on time of flight. A great advantage of this method of separation over a quadrupole mass spectrometer is that a very wide range of masses (m/z 15 to >400) can be measured all at the same time. Another important advantage is the much higher mass resolution which allows the machine to distinguish between ions with very similar m/z values.[16]

[13] Hansel et al., "Proton Transfer Reaction Mass Spectrometry."
[14] Hansel et al., "Proton Transfer Reaction Mass Spectrometry."
[15] Jordan et al., "A High Resolution and High Sensitivity Proton-Transfer-Reaction Time-of-Flight Mass Spectrometer (PTR-TOF-MS)."
[16] Jordan et al., "A High Resolution and High Sensitivity Proton-Transfer-Reaction Time-of-Flight Mass Spectrometer (PTR-TOF-MS)."

2.Material and Methods

2.1 Experiment Nr. 1: Polystyrene

2.1.1 Sampling

The goal of this experiment was to asses polystyrene sensitivity using PTR-MS. Some exploratory measurements with polystyrene had been done before. They showed that the polystyrene mass should be below 250 ng as too much polystyrene at once would pollute the system. To be safe, we started out at masses below 100 ng. In order to accurately and reproducibly sample such small amounts of polystyrene we used a standard; a solution of polystyrene spheres with a diameter (1.046 ± 0.016) µm in water, with a polystyrene mass concentration of 2%.[17]

The target concentrations of the samples were 200, 100, 50, 20, 10, 5, 1, 0.5, 0.2 and 0.1 ng/µL. The first step was mixing standard with Milli-Q water with a ratio of 1:99.7 respectively. This resulted in a concentration of 200 ng/µL from which the rest of the concentrations were made.

The standard was mixed with Milli-Q water using a sterile 5 µL syringe. Further dilutions were done using a 1000 to 100 µL pipette. Some sedimentation of the polystyrene spheres occurred in the 100 to 50 µL samples. To solve this issue, the next bunch of dilutions had volumes of 1 to 0.5 mL.

To measure the polystyrene in a clean environment, glass vials with quartz filters inside were baked at 250^{o} C for at least 12 hours. After these vials with filters cooled down to room temperature, 1 µL of each concentration was loaded onto three filters using a sterile 5 µL syringe. The blanks for this experiment were vials with clean filters inside. System blanks were simply clean, empty vials.

After the loading, the samples along with the blanks and system blanks were dried in an oven at 50^{o} C for two hours. All of the vials were then closed off with new caps, and stored in a refrigerator until they were measured.

For the concentrations above 1 ng/µL, two bunches of vials were made. One was measured using clean ambient air, which was cleaned by running it through a catalyzer at 400^{o} C. The other bunch of samples was measured using pure nitrogen from a pressurized tank. This was done in order to decide which of the two carrier gases would have the least background noise.

The polystyrene measurements were done over the course of four days as shown in the tables below.

Table 1.

Summary of measurements of polystyrene masses 1, 5, 10, 20 and 50 ng

8-4-2019

Nr.	Start	Carrier Gas	Plastic Type	Flow (mL/minute)	Mass (ng)
1	11:19	Air	None (Blank)	50	-
2	11:37	Air	None (Blank)	50	-
3	11:55	Air	Carry Over	50	-
4	12:15	Air	None (System Blank)	50	-
5	12:39	Air	Polystyrene	50	10

[17] According to microParticles GmbH

6	12:59	Air	Polystyrene	50	1
7	13:17	Air	Polystyrene	50	20
8	13:36	Air	Polystyrene	50	50
9	14:09	Air	Carry Over	50	-
10	14:27	Air	Polystyrene	50	5
11	14:45	Air	Polystyrene	50	50
12	15:03	Air	Polystyrene	50	1
13	15:23	Air	Polystyrene	50	5
14	15:42	Air	None (Blank)	50	-
15	15:59	Air	None (System Blank)	50	-
16	16:17	Air	Polystyrene	50	5
17	16:34	Air	Polystyrene	50	50
18	16:53	Air	None (System Blank)	50	-

9-4-2019

Nr.	**Start**	**Carrier Gas**	**Plastic Type**	**Flow (mL/minute)**	**Mass (ng)**
1	11:19	Air	Polystyrene	50	20
2	11:36	Air	Polystyrene	50	10
3	11:55	Air	Polystyrene	50	20
4	12:12	Air	None (Blank)	50	-
5	12:39	Air	Polystyrene	50	1
6	12:57	Air	Polystyrene	50	10
7	13:17	Air	None (Blank)	50	-
8	13:35	Air	None (Blank)	50	-
9	14:09	Air	Polystyrene	50	100
10	14:29	Air	None (System Blank)	50	-

11-4-2019

Nr.	**Start**	**Carrier Gas**	**Plastic Type**	**Flow (mL/minute)**	**Mass (ng)**
1	11:59	Nitrogen	None (Blank)	50	-
2	12:18	Nitrogen	Polystyrene	50	10
3	12:35	Nitrogen	Polystyrene	50	1
4	12:43	Nitrogen	Polystyrene	50	50
5	13:11	Nitrogen	Polystyrene	50	20
6	13:29	Nitrogen	Polystyrene	50	10
7	13:48	Nitrogen	None (Blank)	50	-
8	14:06	Nitrogen	None (System Blank)	50	-
9	14:23	Nitrogen	Polystyrene	50	5
10	14:40	Nitrogen	Polystyrene	50	50
11	14:59	Nitrogen	Polystyrene	50	10
12	15:16	Nitrogen	Polystyrene	50	5
13	15:34	Nitrogen	None (Blank)	50	-

14	15:52	Nitrogen	None (System Blank)	50	-
15	16:09	Nitrogen	Polystyrene	50	1
16	16:27	Nitrogen	Polystyrene	50	1
17	16:46	Nitrogen	None (System Blank)	50	-

12-4-2019

Nr.	Start	Carrier Gas	Plastic Type	Flow (mL/minute)	Mass (ng)
1	10:37	Nitrogen	Polystyrene	50	50
2	10:54	Nitrogen	None (Blank)	50	-
3	11:12	Nitrogen	None (System Blank)	50	-
4	11:29	Nitrogen	Polystyrene	50	20
5	11:47	Nitrogen	Polystyrene	50	20
6	12:05	Nitrogen	Polystyrene	50	5
7	12:23	Nitrogen	None (Blank)	50	-
8	12:42	Nitrogen	None (System Blank)	50	-
9	13:28	Nitrogen	None (System Blank)	50	-
10	13:46	Nitrogen	None (System Blank)	50	-

2.1.2 PTR parameters

Before the measurements can start, the PTR8000 has to warm up for about an hour. System blanks or otherwise clean and empty vials were used for this purpose. After the warm-up period, the system has to be calibrated on two ion peaks that are always in the carrier gas, but not so abundant that they saturate the system. In this experiment, the peaks at m/z 21.022 and 59.049 were used as suggested in the PTRwid manual.[18]

E/N was always kept at about 120 to avoid clustering and fragmentation as much as possible.

<<p-drift is around 2.9 mbar and T-drift (tube!) is around 130 degrees Celsius>>

2.1.3 Thermal Desorption

The dried samples were loaded into the TD unit where they were incubated at 35^{o} C for two minutes, then ramped up to 350^{o} C over the course of five minutes. The samples stay at this temperature for another five minutes, after which they are cooled down to 35^{o} C again by a fan. This smooth ramping is to ensure that desorption of one's sample can also be plotted as a function of temperature.[19]

[18] Holzinger, "PTRwid: A new widget tool for processing PTR-TOF-MS data."

[19] Materić et al., "Brief Communication: Analysis of organic matter in surface snow by PTR-MS – implications for dry deposition dynamics in Alps."

2.2 Experiment Nr. 2: Other plastics

2.2.1 Sampling

For this experiment the samples were taken from larger solid pieces of various plastics; High-Density Polyethylene (HDPE), Low-Density Polyethylene (LDPE), Linear Low-Density Polyethylene (LLDPE), Polyethylene Terephthalate (PET), Polyvinyl Chloride (PVC), Polypropylene Carbonate (PPC), car tire rubber and styrofoam were sampled.

LLDPE, LDPE, HDPE and PPC grains were obtained from pellets of the respective materials using a saw cleaned threefold with Milli-Q water. PET, styrofoam and car tire rubber were sampled from a plastic water bottle, a piece of styrofoam and a piece of car tire respectively. One problem for this experiment was the fact that no means to accurately measure the mass of the plastic grains was available. To get at least a rough estimate of the size of each grain, a Dino-Eye Eyepiece camera mounted onto an optical "Bleeker" microscope was used to take three pictures of three different sides of each particle. The pixel to length ratio was determined using a 1 mm long ruler etched into a glass pane.

These pictures could then be used to estimate the surface area of three different sides of the grain. After taking the photographs, the grains were then loaded into a clean vial and closed off with a new cap. PVC was an outlier since it was delivered in powder form. The powder was made of grains that were about the size of the smallest grains acquired using the saw on other plastics. In order to get different masses of PVC, multiple particles were loaded per vial.

The blanks and system blanks for these measurements were simply empty and clean vials. The cleaning runs were also done using a clean and empty vial.

Table 2.

Summary of measurements of various PET grains.

14-5-2019

Nr.	Start	Carrier Gas	Plastic Type	Flow (mL/minute)	Estimated Mass (ng)
1	10:41	Air	None (Blank)	50	-
2	10:59	Air	None (Blank)	50	-
3	11:18	Air	PET	50	754
4	11:35	Air	None (Cleaning run)	50	-
5	11:52	Air	PET	50	8100
6	12:09	Air	None (Cleaning run)	50	-
7	12:29	Air	PET	50	4952
8	12:46	Air	None (Cleaning run)	50	-
9	13:03	Air	None (Blank)	50	-
10	13:20	Air	None (Blank)	50	-
11	13:37	Air	PET	50	911
12	13:54	Air	None (Cleaning run)	50	-
13	14:10	Air	PET	50	5967

14	14:27	Air	None (Cleaning run)	50	-
15	14:43	Air	PET	50	9393
16	15:00	Air	None (Cleaning run)	50	-
17	15:16	Air	None (Blank)	50	-
18	15:32	Air	None (Blank)	50	-
16-5-2019					
1	10:42	Air	None (Blank)	50	-
2	10:58	Air	None (Blank)	50	-
3	11:15	Air	LDPE	50	1407
4	11:32	Air	None (Cleaning run)	50	-
5	11:48	Air	LDPE	50	4479
6	12:04	Air	None (Cleaning run)	50	-
7	12:23	Air	LDPE	50	1480
8	12:41	Air	None (Cleaning run)	50	-
9	13:00	Air	PVC	50	862
10	13:20	Air	None (Cleaning run)	50	-
11	13:45	Air	PVC	50	1209
12	14:03	Air	None (Cleaning run)	50	-
13	14:21	Air	None (Blank)	50	-
14	14:42	Air	PVC	50	1706
15	15:04	Air	None (Cleaning run)	50	-
16	15:21	Air	None (Blank)	50	-
17	15:41	Air	None (Blank)	50	-

2.2.2 Thermal Desorption

No extra steps between sampling and thermal desorption were needed in this experiment, so in principle, TD could start right after taking the samples.

TD happened in the same manner as the previous experiment. This time the amount of plastic was significantly higher, however. This meant that the $H3O^+$ signal, or the m/z peak 21.022, had to be watched throughout the measuring cycle, as this signal is an indicator for how much plastic is in the carrier gas. Because there is a risk of system pollution when measuring relatively unknown plastic masses, the hydronium signal was watched actively during each measurement run.

Another precaution for the high amount of plastic was to do a cleaning run using an empty, clean vial in between every measurement. This cleaning run was meant to remove any stuck plastic (or carryover) ions from the inlet and drift tube.

2.3 Experiment Nr. 3: Het Water Laboratorium

2.3.1 Sampling

The samples for this experiment came from a Dutch laboratory called “Het Water Laboratorium”. The samples consisted of 1000x preconcentrated water from 26 different sources. The samples that were going to be measured by the PTR-MS were diluted by adding 1 µL of said sample to 10 mL of Milli-Q water using a sterile 5 µL syringe. To measure the samples 1 mL was taken from the dilutions, using a

pipette 1000 to 100 µL pipette with a new tip, and loaded into a clean vial.

2.3.2 The Low-Pressure Evaporator (LPE)

The 1 mL dilutions were prepared for measuring using an LPE. The LPE consists of a glass sphere split into two halves that are sealed off with vacuum grease. The top half of the sphere has a 'chimney', which connects it to the vacuum pump and the nitrogen tank. The gas that goes to the vacuum pump passes through a glass container cooled with liquid nitrogen, where the water vapor is separated from its carrier gas.[20]

For the evaporation sequence the samples, now covered by caps with two holes in them, were brought into the glass sphere at atmospheric pressure. The vacuum pump then lowered the pressure to about 6 mbar and kept it there for the three hours it took for the water to evaporate from the vials. After this, the system was repressurized by slowly filling it with nitrogen from the tank at a rate of about 2 mbar per second. The vials were sealed off afterwards and measured following the same routine as the samples of previous experiments.

Because of time constraints, the data of "Het Water Laboratorium" was not fully processed or analyzed. The focus of this thesis was method evaluation for analysis of microplastic traces, which is why the other experiments were given priority here over these measurements.

2.4 Data processing

The data processing for all experiments was done using PTRwid for integration and time averaging, and excel for background subtracting, calculating standard deviations and applying a Limit of Detection (LOD).[21]

2.4.1 Peak extraction

Before the integration of the mass peaks could start a unified mass list was created using PTRwid. This unified mass list is a normalized list of m/z peaks which allows for easy intercomparison between different runs; if no unified mass list is used, the m/z value assigned to a certain peak will vary slightly for different measurements. After this, the mass peaks are integrated using the "export" routine, which takes several hours. After this routine is done, the "Average and Merge Data" tool was used to average over a certain period. This is done to categorize the data and to decrease the data size considerably. The period chosen for all experiments was the period of T>50^{o} C. This period can be selected by creating an "index file" with the condition AL(1)>2.8. AL(1) is the temperature signal in Volts coming from the thermal desorption unit. 2.8 V roughly corresponds to 50^{o} C. In this index file, the data with T<50^{o} C gets index 300 and the data with T>50^{o} C gets index 100 in the resulting .csv file. Because the TD unit is programmed to stay above 50^{o} C for 600 seconds, only the rows with index 100 and #AVG of around 600 should be kept. The resulting file then contains the signal of every detected ion in ppb. More detailed documentation can be found in R. Holzinger's paper "PTRwid: A new widget tool for processing PTR-

[20] Peacock et al., "Understanding Dissolved Organic Matter Reactivity and Composition in Lakes and Streams Using Proton-Transfer-Reaction Mass Spectrometry (PTR-MS)."
[21] Holzinger, "PTRwid: A new widget tool for processing PTR-TOF-MS data."

TOF-MS data."

2.4.2 Background subtraction and LOD calculation

The rest of the data processing was done in MS Excel, after converting the .csv to a .xlsx file.
To remove the background noise from every peak the value of each peak from the nearest blank was subtracted from that of the samples. After this, the LOD, three times the standard deviation of the blanks, is applied to the resulting set of values; meaning that values greater than the LOD are left as is and the values smaller than the LOD are set to zero. The standard deviation of the blanks is calculated using Excel's STDEV function which uses the "n-1" method suited for samples.
What's left is the concentration of every detected mass in ppb for all measurements.

2.4.3 Mass estimation

In the second experiment, some data processing was needed to estimate the mass of each grain. First off the surface area of three sides of each grain was estimated using ImageJ. The ratio of pixels per mm could be set using the set scale function, after which the surface could be outlined using the freehand selection. The 'measure' utility then calculates the surface area in mm^2.
We then estimated that the grains were roughly spherical and thus calculated the radius from the area using formula (2).

$$r = \left(\frac{A}{4} * \pi\right)^{\frac{1}{2}} \qquad (2)$$

Here, A is the average surface area of the grain and r is the radius of the 'sphere'.
From this the spherical volume could be calculated. Using this estimated volume and the density of the relevant plastic an estimated mass was calculated per grain.

2.4.4 Principal Component Analysis (PCA)

PCA serves as a way to visualize the variance of multi-dimensional data in one or several 2D plots of so-called principal components. A value for each principal component is assigned to each 'data dimension', after which the largest principal components can be plotted against each other for a visualization of the variance in the data. In our case, the data subjected to PCA consists of the averages of the triplicate polystyrene measurements, and all of the measurements of the other plastics. As will be clear later, this adds up to a total of 16 dimensions.
RStudio was used for the PCA calculations and data reading; the command "prcomp" was used to calculate the principal components, which were then plotted using the "ggbiplot" command included in the "ggbiplot" package.

3. Results and Discussion

3.1 Experiment Nr. 1: Polystyrene

In the first experiment drops of 1 µL of the polystyrene concentrations 50, 20, 10, 5 and 1 ng/µL were loaded onto filters in triplicates. Two batches were measured; one using air as the carrier gas and the other using nitrogen. Figure 1 shows the TD temperature and ion 105.069 signals for several runs.

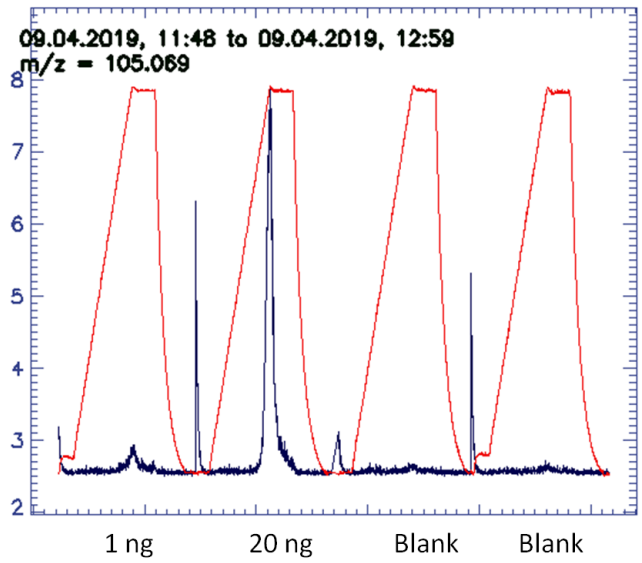

Figure 2: Thermal desorption temperature and ion 105.069 signal for four measurements.
Thermal desorption temperature is shown in red and ion signal is shown in black. Each TD temperature peak represents the duration of a single measurement. Measured polystyrene masses are displayed below the x-axis. The date, time and the m/z of the displayed ion are displayed above.

In figure 2, the time underneath the TD temperature peaks is the time in which the actual measurements take place. In the valleys of these peaks, the vials containing the samples are swapped. During this swap ambient air can flow into the system, which is why there are peaks in the ion signal in between the runs. The first two runs show obvious peaks in the ion 105.069 signal, whereas the blanks are pretty much flat by comparison. The ion signal in the blank runs is not completely flat however; this is the background noise that was mentioned in the data processing section.
One measurement file contains peaks like these, although not as sharp for most m/z values, for over 500 m/z values ranging from 15 to 450. After integrating every peak over the measurement time and averaging over the triplicate measurements, one can plot a full mass spectrum as shown in figure 2.

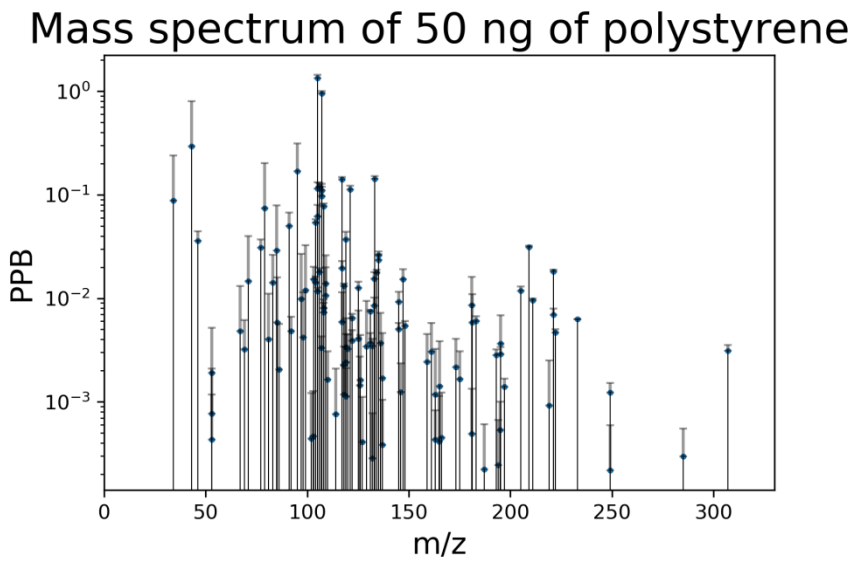

Figure 3. Concentration of ions for 50 ng of PS measured using clean air.

The data comes from three measurements of 50 ng of polystyrene each. The error bars represent the standard deviation of this triplicate measurement. Only positive error bars are shown. A limit of detection of three times the standard deviation of the blanks measured along with these samples has been applied to this plot. All values that were below the LOD are not shown here.

This mass spectrum clearly shows that the PTR-MS system is picking up lots of signals above the detection limit when only 50 ng of polystyrene is measured. Some of the peaks have standard deviations larger than their lengths. These peaks are the result of one of the triplicate measurements having a value above the LOD by chance, and the other two falling below the LOD.

However, most of the peaks have rather small standard deviations of less than ten percent of their lengths. The most notable one of these peaks is the one at an m/z of about 105; it is by far the tallest and it has a fairly small error bar as well. To show how well the PTR-MS system can detect polystyrene, a more elaborate plot of this ion is shown in figure 2.

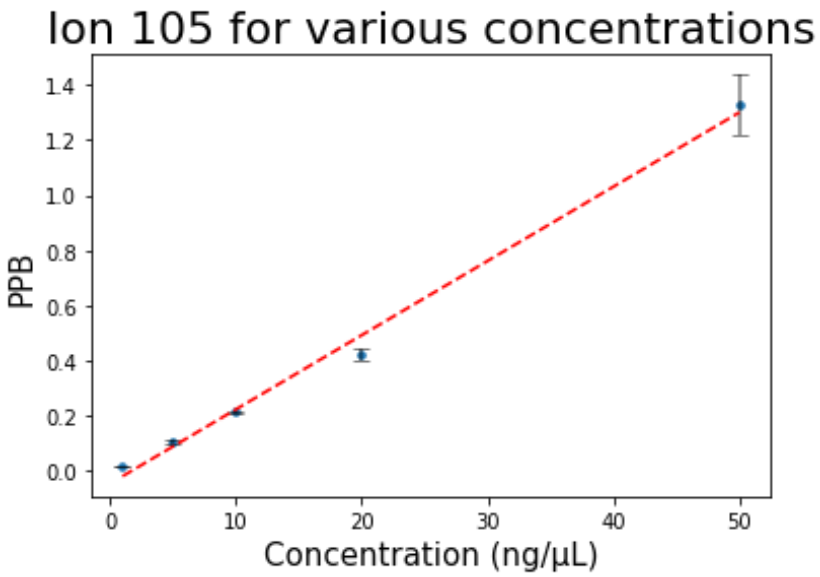

Figure 4. Ion 105 for various polystyrene concentrations.

This plot shows the ppb values of the ion with mass 105.069 plotted against various concentrations of a polystyrene solution in water. 1 µL of each concentration was measured, so the x-axis effectively represents the polystyrene mass. These measurements were done using clean air as the carrier gas. The error bars are the standard deviation of the triplicate measurements of each concentration. The dashed red line is the trend line fitted to the data points.

Figure 4 shows a linear relationship between the measured gas phase concentrations over the thermal desorption time (in ppb) of ion 105.069 and the loaded mass of polystyrene, even down to 1 ng. This ion is plotted because it is the ion with the strongest signal (the highest ppb values). The relationship between the ion 105.069 concentration and the measured polystyrene mass is quite clearly linear. The errors of the measured masses are 6 to 7% of the measured values, with the exception of the 10 ng measurement, which has an error of only 3%. From this it is clear that the TD-PTR-MS system can detect polystyrene masses down to just one nanogram extremely accurately.

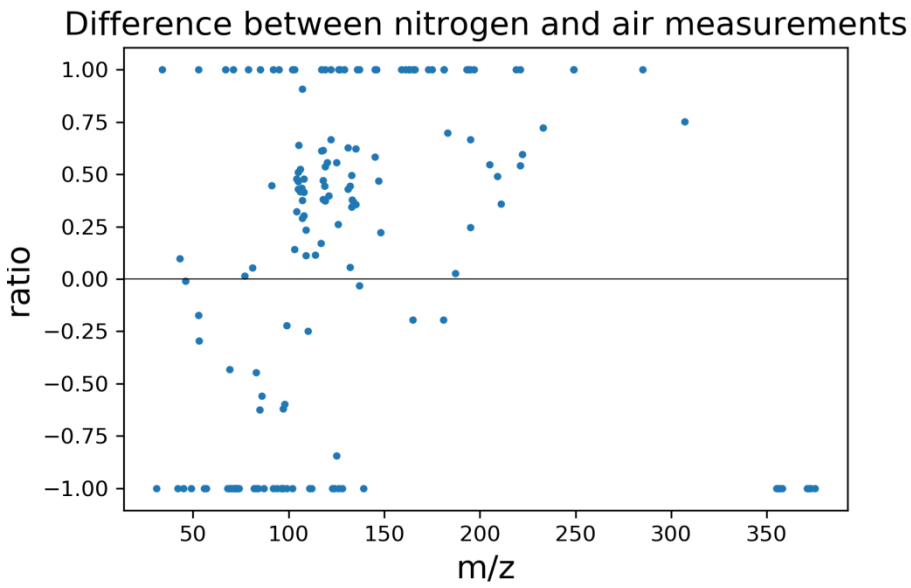

Figure 5. Difference between measurements done on air and nitrogen.

This plot shows the ratio of the difference and the sum of ppb values from the measurements using air and those using nitrogen, plotted against the m/z ratio. The samples that were compared both contained 50 ng of polystyrene.

The "ratio of averages" was calculated for each m/z value using formula (2).

$$r = \frac{X_{air} - X_{N2}}{X_{air} + X_{N2}} \qquad (2)$$

Here, X_{air} is the mean value for air, X_{N2} is the mean value for nitrogen and r is the "ratio of averages". The points below zero represent the ions for which there was a stronger response in the nitrogen measurements than in the air measurements. The points above zero represent ions for which the inverse is true. It is clear that there are significantly more points above than below zero. The points at -1 represent ion signals which were above the LOD in the nitrogen measurements but below the LOD in the air measurements. The points at +1 represent the inverse.

The fact that there are far more points above zero in figure 5 than below zero indicates that the nitrogen blanks have a higher limit of detection than the air blanks, or that nitrogen simply picks up fewer ions than air during thermal desorption.

It is possible that the reason for the difference in results lies within the different physical properties of the two carrier gases. For instance, nitrogen is a slower and less reactive gas than oxygen. The slower nitrogen could lose more ions on the walls of the inlet than air would. However, since air consists mostly of nitrogen already, this difference in speed should not result in such a major difference in result.

Another possible reason is that the zero air was simply much warmer than the nitrogen as it was being pumped through the vial containing the sample. This is because the nitrogen comes from a tank with compressed nitrogen, so as the nitrogen exits this high-pressure environment, it loses heat. A colder carrier gas picks up fewer particles, resulting in lower ppb values for the nitrogen measurements than for the air measurements.

Yet another potential reason for the difference in outcomes of the two sets of experiments is oxygen's role in desorption of the plastics. The pure nitrogen does, of course, not contain any oxygen. The clean air, on the other hand, is made up of about 20% oxygen.

3.2 Experiment 2.1: PET

In this experiment, six PET grains of various sizes were measured in order to test the accuracy of the mass estimates.

Figure 6. Images of each measured grain with the corresponding estimated masses.
These images were taken with a camera mounted onto a microscope. Seen in black in the image are grains of PET with rather irregular shapes lying on a glass pane. The smaller, vague shapes in the images are dust particles on the lens of the microscope. The sharp smaller shapes are either dust particles or bits of plastic that fell off of the larger grains. The number above each image represents the estimated mass of the grain. The image at the bottom is a photo of a 1mm long ruler etched into a glass pane. This is to indicate the scale for the rest of the images.

Figure 6 clearly shows that none of the PET grains are particularly sphere-like, apart from perhaps the particle in the bottom right corner. In fact, it seems like the grains are better approximated by a rod-like or cylindrical shape.
The grain shown in the bottom left with estimated mass of 5967.22 ng stood out. It is slightly more transparent than the other grains, and subsequent pictures do not show a significantly different surface

like with the rest of the particles. All three of the images of this grain are shown below in figure 7.

Figure 7. Three images of the grain with estimated mass m= 5967.22 ng

These images were taken with a camera mounted onto a microscope. The large black shapes are three different orientations of a certain grain of PET. The grain was flipped in between each photo in order to capture multiple sides of the grain's surface. All three pictures seem to be of the same side.

The other photos of this particular grain were simply the same shape rotated in the plane of the glass pane. This means that the particle likely was rather flat; a more round particle would show different sides of itself upon being flipped. Because it was assumed that the grains were approximately spherical when estimating their masses, this likely resulted in a strong overestimation of the mass.

Figure 8. Ions 105 and 123 for the six measured PET grains.

The plot on the left shows the concentration of the ion with m/z 105.069 in ppb plotted against the mass of the relevant PET grain in ng. The plot on the right shows the concentration of the ion with m/z 123.44 in ppb plotted against the mass of the relevant PET grain in ng. The red lines are linear trend lines fitted to the actual data. These ions, in particular, are shown because they are two of the most abundant characteristic ions for PET.

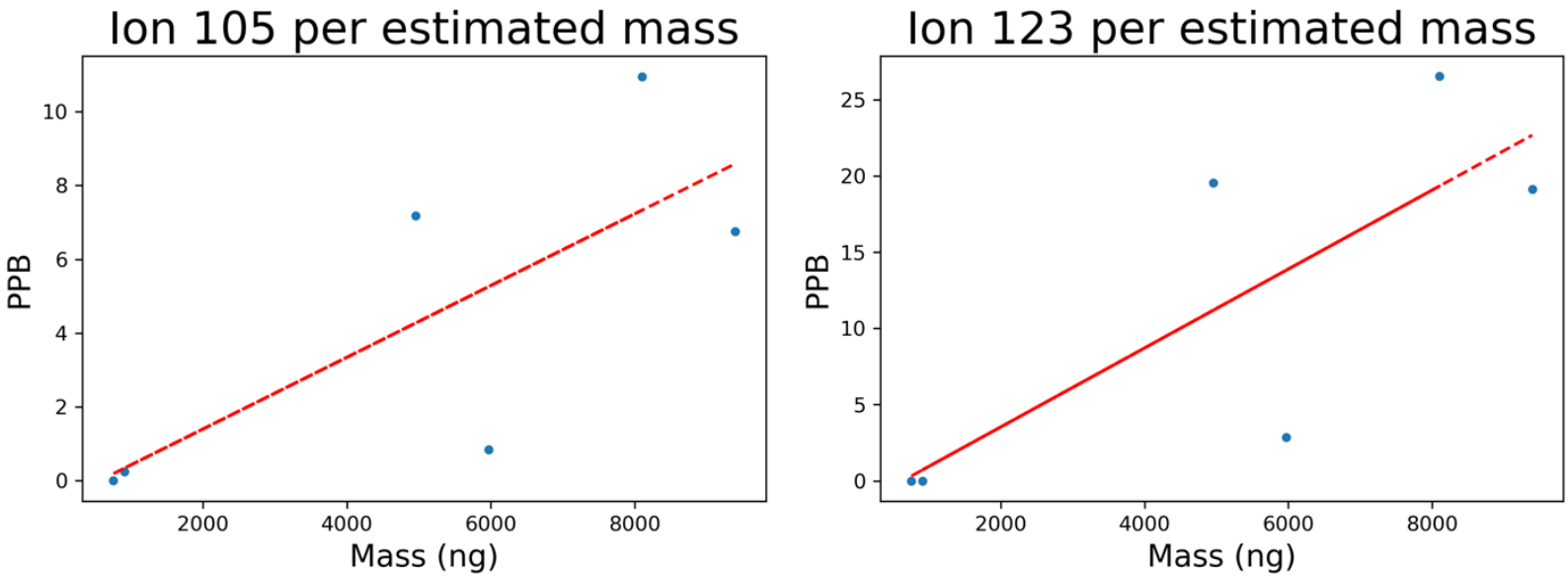

The data on the left side of Figure 8 has an R-squared value of 0.5787 and the data on the right has an R-squared value of 0.6205. At an R-squared of about 0.75 or higher one could still argue for a linear relationship in the plots. Therefore this is the case for neither of the two plots. However, as explained in the prior section, one grain's mass was severely overestimated. In addition to this, in the plot on the right, the two lowest masses did not go above the limit of detection. This is strange because even the lower PET masses are much higher than the measured polystyrene masses, so one would expect the characteristic ions to make it above the LOD.

Upon closer inspection of the data, it seems that the problem lies with the limit of detection. As was previously mentioned, some of the ions coming from the heated plastic get stuck to the inlet and drift tube. Because such high amounts of plastic were measured in this experiment, cleaning runs were done in between each measurement to get rid of the stuck ions. However, it seems that so many ions got stuck that the blanks were also affected by them. For instance, the first two blanks that were run before the measurements had an ion 123 signal of about 0.0170 and 0.0176 ppb. Two subsequent blanks that were run after a cleaning run had an ion 123 signal of about 0.7 and 0.3 ppb; one order of magnitude higher. This is almost certainly because of the carryover from the measurement that was run before the cleaning run.

Because the ion 123 signals of the smallest grains are smaller than one, they were filtered out by the enlarged limit of detection. Because the LOD was likely bloated by stuck ions from a big grain, this does not necessarily mean that the PTR-MS apparatus did not pick up their signals. Leaving out the overestimated grain and inserting the measured values for the two lowest masses results in R-squared values of 0.7723 and 0.816 instead. These R-squared values do indicate that a linear relationship is present, and thus that the spherical approximation may tentatively be used to plot concentrations against estimated masses.

3.3 Experiment 2.2: LDPE

Due to the lack of success in estimating the mass of plastic grains using photos of the surface, the idea of plotting the ppb-mass relation for each kind of plastic was less important, so fewer samples were measured than in the PET experiment. To test whether the PTR-MS apparatus can distinguish between the other plastic types and to build a library of plastic signatures, the rest of the plastics were measured in triplicates.

The LDPE measurements showed some very strong signals around 61 m/z. Most notable was the ion with mass 61.028; the largest grain gave off over 36 ppb. For the smaller grains, the values are significantly smaller, but only vaguely proportional to the estimated mass. This again shows the inaccuracy of the spherical approximation of the grains.

The PVC measurements also showed some signals significantly above the limit of detection, of which the largest signal was found at 79.052. The largest PVC mass which consisted of five grains of the powder gave off over 18 ppb of this ion.

It was expected that the sphere approximation would work the best for the PVC grains since they looked rather round in the microscope. Sadly the ppb value of one of the samples is always some large negative value when the other two measurements show a strong signal. This issue is likely caused by some rather large background noise during this measurement. Because of this unusable measurement it is impossible to look for any linear relationship between ppb and mass.
A summary of the findings of this experiment is shown below in the boxplots.

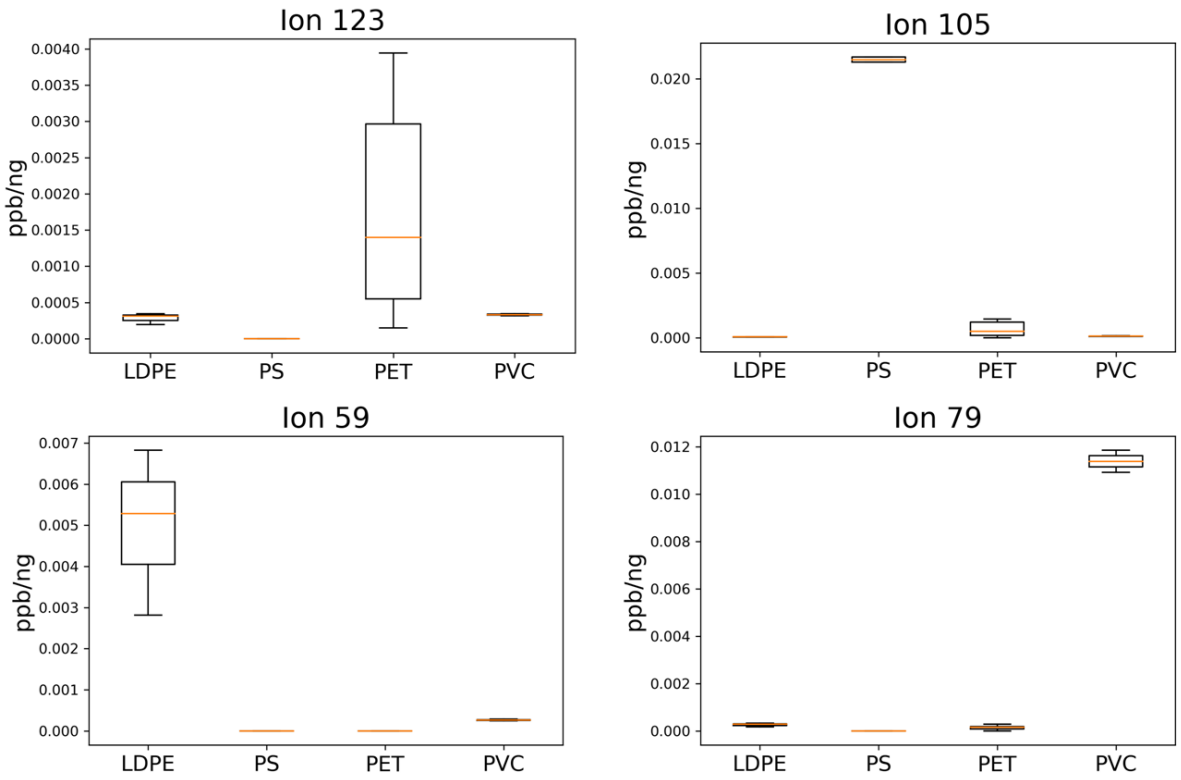

Figure 9: Boxplots of several ions for each measured plastic type

This figure shows boxplots of the concentration of a certain ion in ppb divided by the plastic mass for the four measured plastic types. The ions were chosen so that for each ion there is one plastic that gives off a vastly higher signal than the other three.

From figure 9 it is clear that each of the four plastic types has at least one ion that it emits far more than the others during thermal desorption. The boxplot of PET looks so stretched due to previously discussed issues with the limit of detection.
Finding all of the ions that have this property for a given plastic could perhaps be used to detect this plastic in a sample containing a mix of several different plastic types.

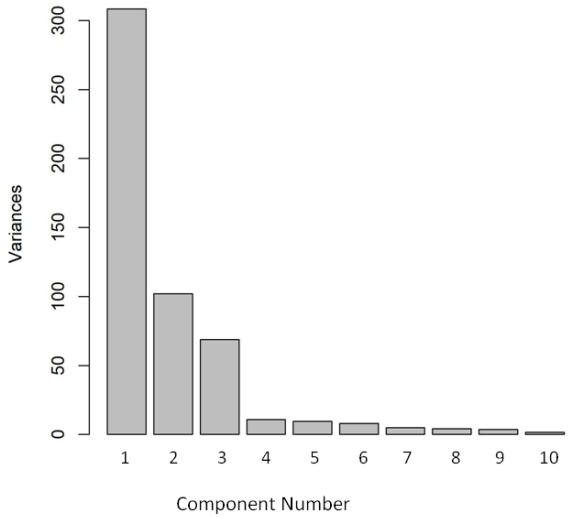

Figure 10: Scree plot of the principal components

Here, the variances are shown for the first ten principal components. Each component is smaller than the previous, so the last six were left out.

The first step in PCA is to check whether the principal components are a reasonable representation for the variance of the data. To do this, a scree plot was generated for the measured ions in the range m/z=20.023 to m/z=449.087. From the scree plot it seems that the first three principal components account for the vast majority of the variance in the data, so plotting them against one another should give a good visual representation of these variances. Further calculations show that the first three components indeed account for around 90% of the variance in the data, depending on the range of selected ions. Detailed results of the PCA are shown below.

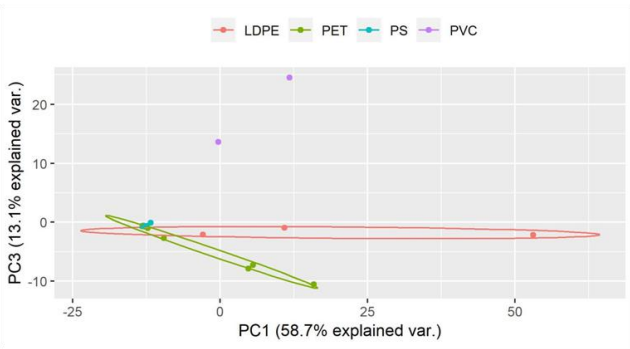

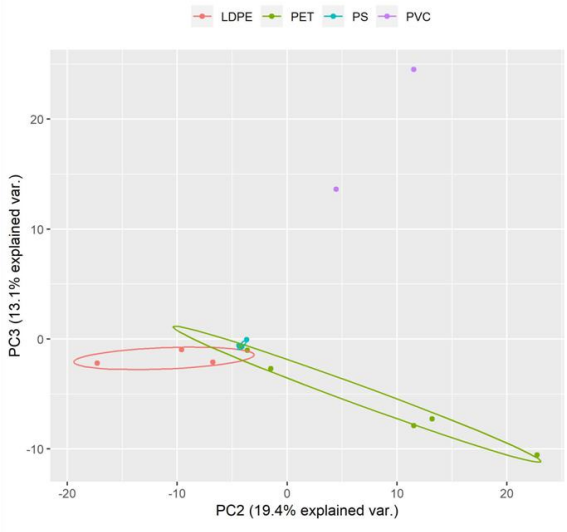

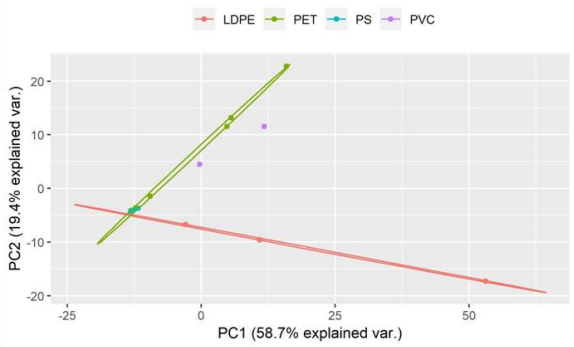

Figure 11: Plots of principal components 1, 2 and 3 for all detected ions

The points in the plot represent the value of the displayed principal components for a certain measured sample. All detected ions were taken into account for these plots. The polystyrene points are the averages of the triplicate measurements. The axis labels also display the percentage of the variance that each principal component accounts for, in parentheses.

Figure 11 shows the first three principal components plotted against each other, which were calculated from the plastic sample data with the background subtracted and LOD applied. The plots show that PVC is clearly separated from the rest. However, the LDPE and PET regions have some overlap with each other and with the PS points.

Similar plots were created using different ranges of ion masses, for instance only ions with m/z greater than 100. Changing the range did not improve the separation between the different plastic types however. Thus, it seems that PCA cannot distinguish between PET, LPDE and PS very well if only the raw ppb values are known.

One reason for this may be the vastly different mass ranges that were measured for the plastic types; 1 to 50 ng of PS was measured, whereas the estimated PET masses range from 700 to 9000 ng. Because this was not accounted for in any way in the PCA above, the variance of PS is much smaller than that of the other plastics. Compensating for the difference in mass may therefore result in improved separation in the PCA plots. Plots of this mass compensated data are shown below.

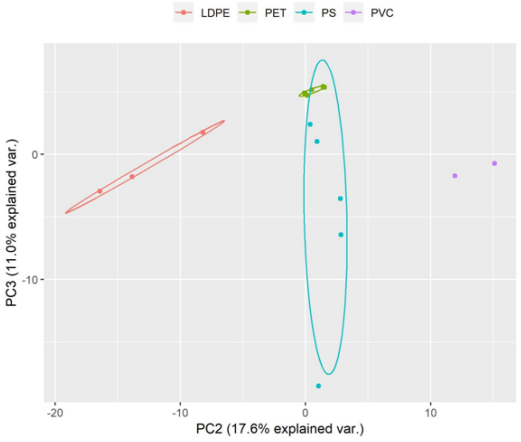

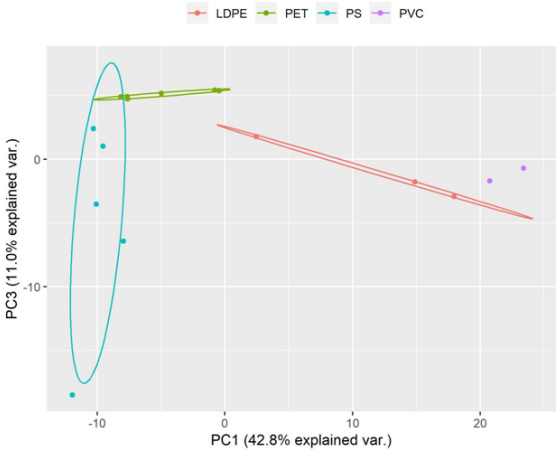

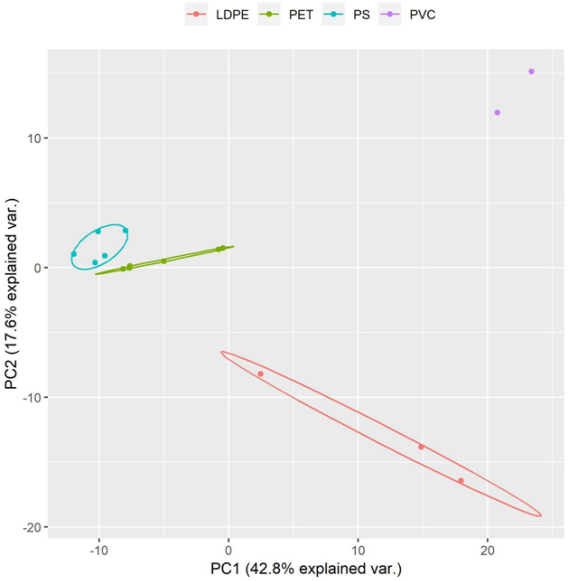

Figure 12: Plots of principal components 1,2 and 3 for ions with m/z greater than 100
The data plotted here is the same as in figure 11, but the ppb values of each sample have been divided by the measured plastic mass. Also, all ions with m/z less than 100 were left out.

Accounting for the different measured masses does have two downsides. Firstly, one has to know the plastic masses that are being measured or at least the ratios between them, which is not always the case for environmental samples. Secondly, the first three principal components now represent only 70% of the variance, down from 90% in the analysis of the raw data. This is still the majority of the variance. However, it is less certain that the principal component plots are a good representation of the data variance.
That said, there is also a clear advantage. As shown in figure 12, LDPE and PET are now nicely separated. PS and PET still have some overlap, but far less than in figure 11, and they are even separate in the plot of the largest two principal components.
As discussed before, the PET data suffers from both an inflated limit of detection and inaccurate mass estimation. These issues likely make the PET region in the PCA plots much less compact than it could be. It is therefore not certain that PET will overlap with PS or LDPE for data with clean blanks and accurate mass estimates.

4. Conclusion and outlook

In this thesis, we tested a method for analysis of microplastic traces using TD-PTR-TOF-MS. The first experiment showed that the PTR-MS apparatus can measure polystyrene masses as small as one nanogram with an error of less than one ppb. The second experiment showed that it is also possible to detect and distinguish between PS, PET, LDPE, and PVC using the PTR-MS system. This was done using principal component analysis. These results strongly imply that, if they exist, microplastic traces can also be found in environmental and atmospheric samples using PTR-MS.

The measurements of larger quantities of plastic could be greatly improved by doing additional cleaning runs in between measurements. This would significantly lower the effect that high plastic masses have on subsequent blanks and other measurements.

The obvious next step is to expand the library of plastics further so that every plastic may be identified via fingerprinting. The lower limit of plastic mass that can be detected by PTR-MS is also something that should be researched further. To potentially push the limit of detection even lower, other carrier gases such as Helium could be tested in future research. The usefulness of PCA may also be further researched by measuring the other plastics with clean blanks. This would allow for tighter grouping of the plastic types in the principal component plots.

Once the method is up to the desired standards, measurements on environmental samples such as drinking water and alpine snow could be tested for microplastic traces.

Bibliography

"First Overview of Microplastics in Indoor and Outdoor Air." ResearchGate. Accessed April 7, 2019. https://www.researchgate.net/publication/281657363_First_overview_of_microplastics_in_indoor_and_outdoor_air.

Allen, Steve, Deonie Allen, Vernon R. Phoenix, Gaël Le Roux, Pilar Durántez Jiménez, Anaëlle Simonneau, Stéphane Binet, and Didier Galop. "Atmospheric Transport and Deposition of Microplastics in a Remote Mountain Catchment." *Nature Geoscience* 12, no. 5 (May 2019): 339–44. https://doi.org/10.1038/s41561-019-0335-5.

Andrady, Anthony L. "Microplastics in the Marine Environment." *Marine Pollution Bulletin* 62, no. 8 (August 1, 2011): 1596–1605. https://doi.org/10.1016/j.marpolbul.2011.05.030.

Cox, Kieran D., Garth A. Covernton, Hailey L. Davies, John F. Dower, Francis Juanes, and Sarah E. Dudas. "Human Consumption of Microplastics." *Environmental Science & Technology*, June 5, 2019. https://doi.org/10.1021/acs.est.9b01517.

Hansel, A., A. Jordan, R. Holzinger, P. Prazeller, W. Vogel, and W. Lindinger. "Proton Transfer Reaction Mass Spectrometry: On-Line Trace Gas Analysis at the Ppb Level." *International Journal of Mass Spectrometry and Ion Processes* 149–150 (November 1995): 609–19. https://doi.org/10.1016/0168-1176(95)04294-U.

Jambeck, Jenna R, Roland Geyer, Chris Wilcox, Theodore R Siegler, Miriam Perryman, Anthony Andrady, Ramani Narayan, and Kara Lavender Law. "Plastic Waste Inputs from Land into the Ocean," n.d., 5.

Jordan, A., S. Haidacher, G. Hanel, E. Hartungen, L. Märk, H. Seehauser, R. Schottkowsky, P. Sulzer, and T.D. Märk. "A High Resolution and High Sensitivity Proton-Transfer-Reaction Time-of-Flight Mass Spectrometer (PTR-TOF-MS)." *International Journal of Mass Spectrometry* 286, no. 2–3 (September 2009): 122–28. https://doi.org/10.1016/j.ijms.2009.07.005.

Käppler, Andrea, Dieter Fischer, Sonja Oberbeckmann, Gerald Schernewski, Matthias Labrenz, Klaus-Jochen Eichhorn, and Brigitte Voit. "Analysis of Environmental Microplastics by Vibrational Microspectroscopy: FTIR, Raman or Both?" *Analytical and Bioanalytical Chemistry* 408, no. 29 (November 2016): 8377–91. https://doi.org/10.1007/s00216-016-9956-3.

Li, W. C., H. F. Tse, and L. Fok. "Plastic Waste in the Marine Environment: A Review of Sources, Occurrence and Effects." *Science of The Total Environment* 566–567 (October 1, 2016): 333–49. https://doi.org/10.1016/j.scitotenv.2016.05.084.

Löder, Martin G. J., and Gunnar Gerdts. "Methodology Used for the Detection and Identification of Microplastics—A Critical Appraisal." In *Marine Anthropogenic Litter*, edited by Melanie Bergmann, Lars Gutow, and Michael Klages, 201–27. Cham: Springer International Publishing, 2015. https://doi.org/10.1007/978-3-319-16510-3_8.

Materić, Elke Ludewig, Kangming Xu, Thomas Röckmann, and Rupert Holzinger. “Brief Communication: Analysis of Organic Matter in Surface Snow by PTR-MS – Implications for Dry Deposition Dynamics in the Alps.” *The Cryosphere* 13, no. 1 (January 30, 2019): 297–307. https://doi.org/10.5194/tc-13-297-2019.

Bauerlein, Dekker, Koelmans.“Closing the Gap between Small and Smaller: Towards a Framework to Analyse Nano- and Microplastics in Aqueous Environmental Samples.” ResearchGate. Accessed May 26, 2019. https://www.researchgate.net/publication/325410540_Closing_the_gap_between_small_and_smaller_Towards_a_framework_to_analyse_nano-_and_microplastics_in_aqueous_environmental_samples.

Holzinger. “PTRwid: A New Widget-Tool for Processing PTR-TOF-MS Data.” ResearchGate. Accessed June 10, 2019. https://www.researchgate.net/publication/272389949_PTRwid_a_new_widget-tool_for_processing_PTR-TOF-MS_data.

Peacock, Mike, Dušan Materić, Dolly N. Kothawala, Rupert Holzinger, and Martyn N. Futter. “Understanding Dissolved Organic Matter Reactivity and Composition in Lakes and Streams Using Proton-Transfer-Reaction Mass Spectrometry (PTR-MS).” *Environmental Science & Technology Letters* 5, no. 12 (December 11, 2018): 739–44. https://doi.org/10.1021/acs.estlett.8b00529.

Webb, Hayden K., Jaimys Arnott, Russell J. Crawford, and Elena P. Ivanova. “Plastic Degradation and Its Environmental Implications with Special Reference to Poly(Ethylene Terephthalate).” *Polymers* 5, no. 1 (March 2013): 1–18. https://doi.org/10.3390/polym5010001.